

Department of Pharmacology¹, Department of Natural Medicines², Faculty of Pharmacy, Takasaki University of Health and Welfare, Gunma, Japan

Neurite outgrowth promotion in PC12 cells by 24(*R*)-ethyllophenol from *Morus alba*

S. HONMA^{1,*}, K. HANDA¹, R. MITSUMATA¹, D. SHIMADA¹, S. TAKEI¹, G. TANAKA¹, K. WATANABE², M. YOSHIDA¹

Received November 14, 2023, accepted May 5, 2024

*Corresponding author: Shigeyoshi Honma, Ph. D., Department of Pharmacology, Faculty of Pharmacy, Takasaki University of Health and Welfare, 60 Nakaorui-machi, Takasaki Gunma 370-0033, Japan
shonma@takasaki-u.ac.jp

Pharmazie 79: 67-71 (2024)

doi: 10.1691/ph.2024.3656

We examined the mechanism by which 24(*R*)-ethyllophenol (MAB28) isolated from the branches of *Morus alba* caused neurite outgrowth in rat pheochromocytoma cells (PC12). MAB28 significantly promoted neurite outgrowth to a similar degree as the positive control, nerve growth factor (NGF). After incubation with MAB28 in PC12 cells, phosphorylation of extracellular signal-regulated kinase, p38 mitogen-activated protein kinase, and cyclic AMP response element-binding protein was detected, but the time course of phosphorylation was different from that induced by NGF. The expression of chloride intracellular channel protein 3 (CLIC3) was significantly decreased by MAB28. 5-Nitro-2-(3-phenylpropylamino)-benzoic acid (NPPB), an outward rectifying chloride channel inhibitor, significantly promoted neurite outgrowth in PC12 cells. These data suggested that MAB28 could induce neurite outgrowth by downregulating CLIC3 expression.

1. Introduction

Neurotrophic factor is a general term for substances that promote survival, differentiation, and regeneration of nerve cells, among which nerve growth factor (NGF) is the most representative factor. Rat pheochromocytoma cells (PC12) have been used in many studies because they respond to NGF, which induces neuron-like differentiation. Two receptors bind NGF: the high-affinity tropomyosin receptor kinase (Trk) A receptor and the low-affinity p75 neurotrophin receptor. Binding of NGF to the TrkA receptor induces receptor dimerization and autophosphorylation of the receptor due to its tyrosine kinase activity. The binding of various proteins to the phosphorylated TrkA receptor activates mitogen-activated protein kinase (MAPK) and cyclic AMP response element-binding protein (CREB), which are involved in the differentiation of PC12 cells (Ginty et al. 1994; Morooka and Nishida 1998). However, because neurotrophic factors such as NGF are high-molecular proteins and cannot penetrate the blood-brain barrier even when administered from the periphery, they cannot enter the brain. Therefore, the development of low-molecular-weight compounds exhibiting NGF-like action is under way.

Morus alba L. (Moraceae) is used not only as a food plant for silkworms but also as a traditional herbal medicine and functional food. Its leaves have antidiabetic (Evans et al. 1985) and antihypertensive effects (Naowaboot et al. 2009); its root bark has anti-hyperlipidemia (El-Beshbishy et al. 2006) and whitening effects (Kim et al. 2010); its fruit constituents have antitumor (Chen et al. 2006) and antithrombotic activities (Yamamoto et al. 2006); and its branches have antidiabetic activity (Ahn et al. 2017). However, little is known about the biological activities of the chemical constituents of the branches of *M. alba* compared to those of the other parts such as leaves, root bark, and fruits.

In our knowledge, this is the first report that demonstrate the effect of 24(*R*)-ethyllophenol (MAB28), isolated from the branches of *M. alba*, on neurite outgrowth in PC12 cells (Fig. 1). The present study was undertaken to investigate the mechanism by which MAB28 promotes neurite outgrowth. Our findings indicate that MAB28 may induce neurite outgrowth by downregulating chloride intracellular channel protein 3 (CLIC3) expression.

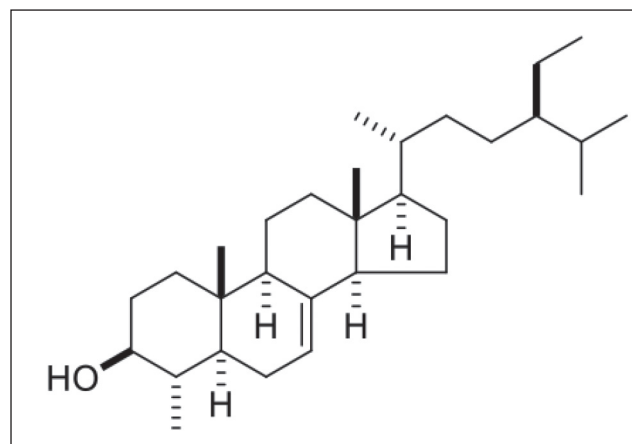


Fig. 1: Chemical structure of 24(*R*)-ethyllophenol (MAB28)

2. Investigations and results

2.1. Effect of MAB28 on neurite outgrowth in PC12 cells

PC12 cells were treated with 10–100 μ M MAB28 for 1 or 2 days and phase-contrast microscopy used to assess morphological changes. MAB28 and NGF (positive control) promoted neurite outgrowth in PC12 cells (Fig. 2A). The differentiation scores of the neurite-bearing cells revealed that treatment with 30 and 100 μ M MAB28 for 2 days significantly promoted neurite outgrowth to a similar degree as NGF (Fig. 2B).

2.2. MAB28 causes phosphorylation of ERK, p38MAPK, and CREB

NGF is known to induce phosphorylation of ERK, p38MAPK, and CREB in PC12 cells (Ginty et al. 1994; Marshall 1995; Morooka and Nishida 1998). Therefore, we investigated the phosphorylation of these proteins after MAB28 stimulation. Treatment with MAB28 (100 μ M) for 2 min significantly increased levels of

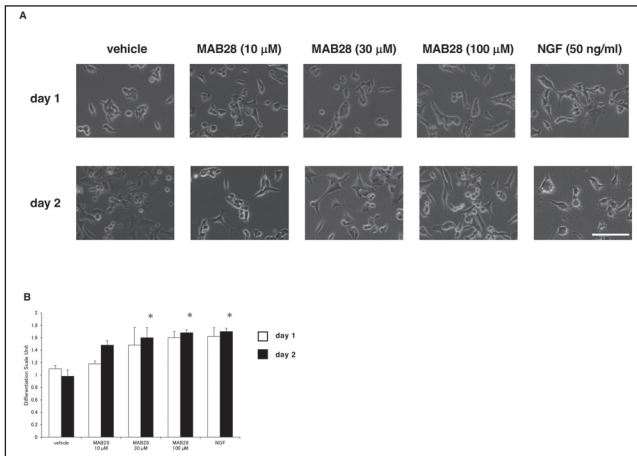


Fig. 2: Effect of MAB28 on neurite outgrowth in PC12 cells. (A) PC12 cells were stimulated with vehicle, MAB28 (10 μ M), MAB28 (30 μ M), MAB28 (100 μ M), or NGF (50 ng/mL) for 1 day (upper row) or 2 days (lower row). Scale bar: 100 μ m. (B) Evaluation of differentiation scores of PC12 cells. The differentiation of PC12 cells was evaluated as described under MATERIALS AND METHODS, and the experiments were performed as shown in Fig. 2A. Data are means \pm S.E.M. (n=4-5). *Significantly different from vehicle at $P < 0.05$.

phospho-ERK (Fig. 3A) and phospho-p38MAPK with a peak at 10 min (Fig. 3B). Phosphorylation of CREB was also significantly increased 2 min after MAB28 addition (Fig. 3C). NGF also caused phosphorylation of ERK, p38MAPK, and CREB, however, the time course of phosphorylation was different from that observed with MAB28 (Fig. 3D-F).

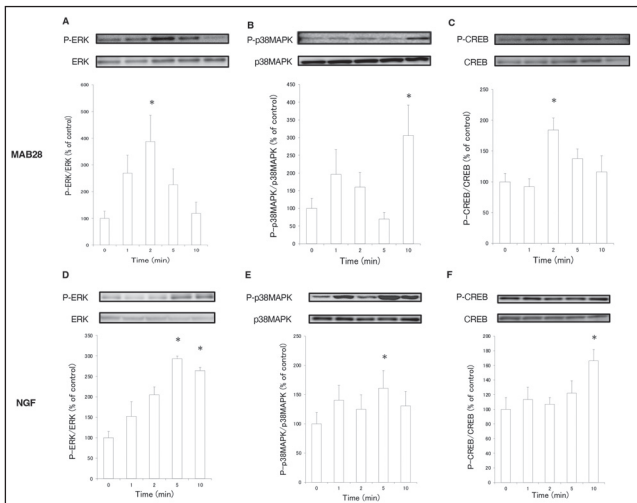


Fig. 3: Effects of MAB28 and NGF on the phosphorylation of ERK, p38MAPK, and CREB in PC12 cells. Samples obtained from PC12 cells treated with MAB28 (100 μ M) (A-C) or NGF (50 ng/mL) (D-F) were separated by SDS-PAGE followed by western blotting with antibodies against ERK or phospho-ERK (A, D), p38MAPK or phospho-p38MAPK (B, E), CREB or phospho-CREB antibodies (C, F). Phosphorylation was normalized to the total levels of ERK, p38MAPK, or CREB and presented as a percentage of vehicle. Data are means \pm SEM. (n=3-5). *Significantly different from vehicle at $P < 0.05$.

2.3. MAB28 decreases CLIC3 mRNA and protein levels

We performed transcriptome and proteome analyses with or without MAB28 stimulation and focused on WD repeat domain 18 (WDR18), CLIC3, and internexin neuronal intermediate filament protein alpha (INA). WDR18 belongs to the WD repeat protein family and plays roles in various biological processes involving the cytoskeleton organization, intracellular transport, mRNA splicing, transcriptional regulation, and cell migration in eukaryotes (Gao et al. 2011). CLIC3 is a member of the CLIC family of proteins consisting of CLIC1 to CLIC6, which are primarily involved in macrophage activation, regulation of intracellular pH, and apoptosis (Chen et al. 2020). INA is a 66-kDa protein that

copurifies with intermediate filaments from rat spinal cord and optic nerve (Kaplan et al. 1990). Transcriptome and proteome analyses revealed that WDR18 and CLIC3 expression was greatly decreased while INA expression was greatly increased by MAB28 stimulation. We performed real-time PCR to confirm that only CLIC3 expression was significantly decreased by MAB28 stimulation, which was consistent with the results obtained by transcriptome analysis (Fig. 4A-C). NGF stimulation did not change the RNA levels of WDR18, CLIC3, or INA (Fig. 4D-F). Further, we also found a significant reduction in CLIC3 protein levels after incubation with MAB28 for 2 days (Fig. 5).

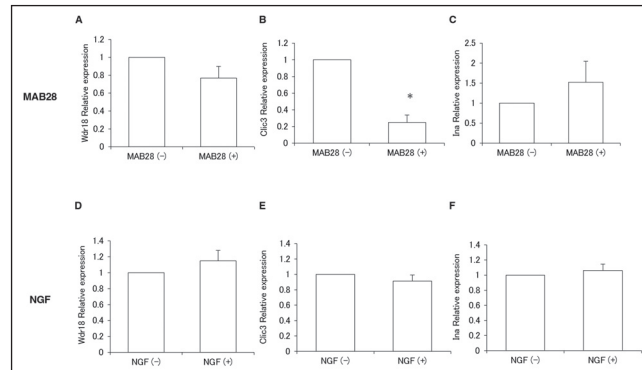


Fig. 4: Real-time RT-PCR analysis of WDR18 (A, D), CLIC3 (B, E), INA (C, F) expression in PC12 cells treated with MAB28 (100 μ M) (A-C) or NGF (50 ng/mL) (D-F) for 1 day. Data are mean \pm S.E.M (n=6). *Significantly different from vehicle at $P < 0.05$.

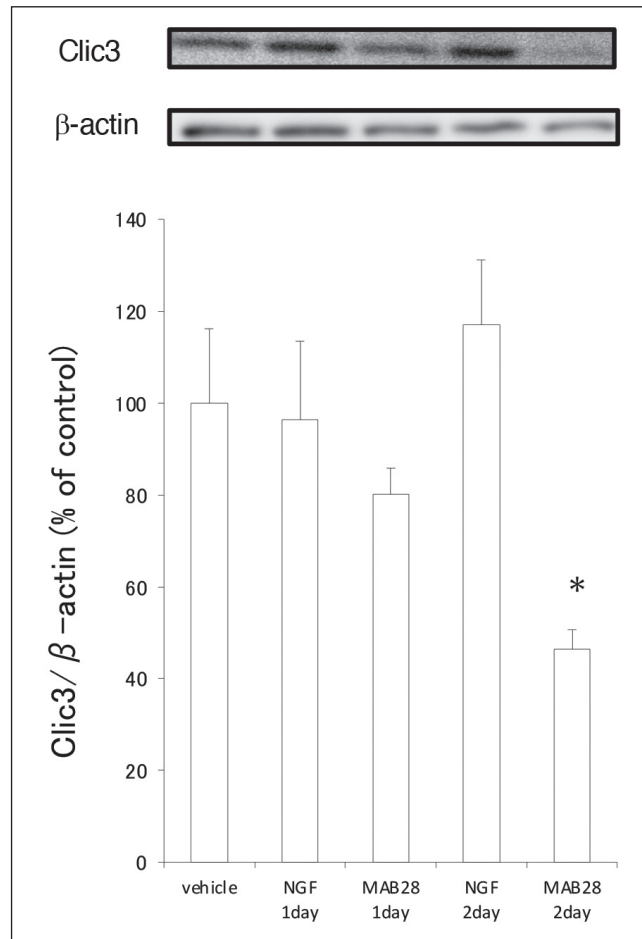


Fig. 5: Effect of MAB28 (100 μ M) or NGF (50 ng/mL) for 1 or 2 days on the expression of CLIC3 in PC12 cells. Samples were separated by SDS-PAGE followed by western blotting with antibodies against CLIC3. The expression level was normalized to the corresponding β -actin level and presented as a percentage of vehicle. Data are mean \pm S.E.M (n=4). *Significantly different from vehicle at $P < 0.05$.

2.4. Inhibition of outward chloride ion channels promotes neurite outgrowth in PC12 cells

As CLIC3 functions as an outward rectifying chloride channel (Kawai et al. 2020), we investigated the effects of NPPB, an outward rectifying chloride channel inhibitor, on neurite outgrowth. PC12 cells were cultured with different NPPB concentrations for 2 days and phase-contrast microscopy used to assess morphological changes (Fig. 6A–F). The differentiation scores of the neurite-bearing cells revealed that 100 nM to 10 μ M of NPPB significantly promoted neurite outgrowth (Fig. 6G).

2.5. Overexpression of CLIC3 inhibits MAB28-induced neurite outgrowth in PC12 cells

It is assumed that MAB28 induce neurite outgrowth by downregulating CLIC3 expression, we next examined its effect on PC12 cells under an overexpression of CLIC3. The differentiation scores of the neurite-bearing cells revealed that overexpression of CLIC3 significantly inhibits MAB28-induced neurite outgrowth (Fig. 7B and C).

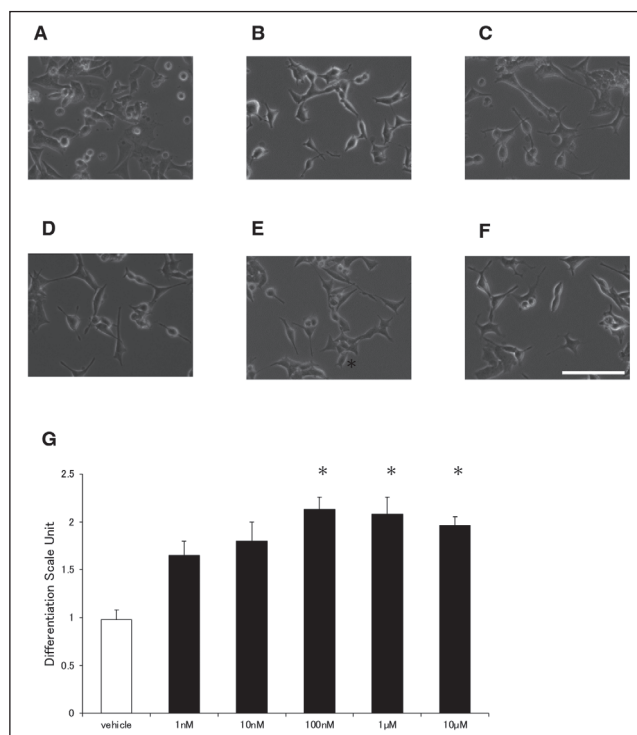


Fig. 6: Effect of NPPB on neurite outgrowth in PC12 cells. PC12 cells were stimulated with vehicle (A), NPPB (1 nM) (B), NPPB (10 nM) (C), NPPB (100 nM) (D), NPPB (1 μ M) (E), or NPPB (10 μ M) (F) for 2 days. Scale bar: 100 μ m. (G) Evaluation of differentiation scores of PC12 cells. The differentiation of PC12 cells was evaluated as described under MATERIALS AND METHODS, and the experiments were performed as shown in Fig. 6A–F. Data are means \pm S.E.M. (n=4–5). *Significantly different from vehicle at $P < 0.05$.

3. Discussion

This work showed that MAB28 isolated from the branches of *M. alba* caused neurite outgrowth in PC12 cells by decreasing the expression of CLIC3. MAB28 increased neurite outgrowth in a dose-dependent manner, similar to the positive control, NGF. Moreover, MAB28 induced the phosphorylation of ERK, p38MAPK, and CREB in PC12 cells, but the peak time of phosphorylation was different from that observed with NGF stimulation. Stimulation of PC12 cells with NGF induces neurite outgrowth, whereas stimulation with EGF induces cell proliferation (Marshall 1995). The differentiation of PC12 cells correlates with sustained activation of ERK. However, blocking this sustained ERK activation does not suppress NGF-induced neurite outgrowth (York et al. 1998). Thus, given that the signals inducing ERK activation are diverse,

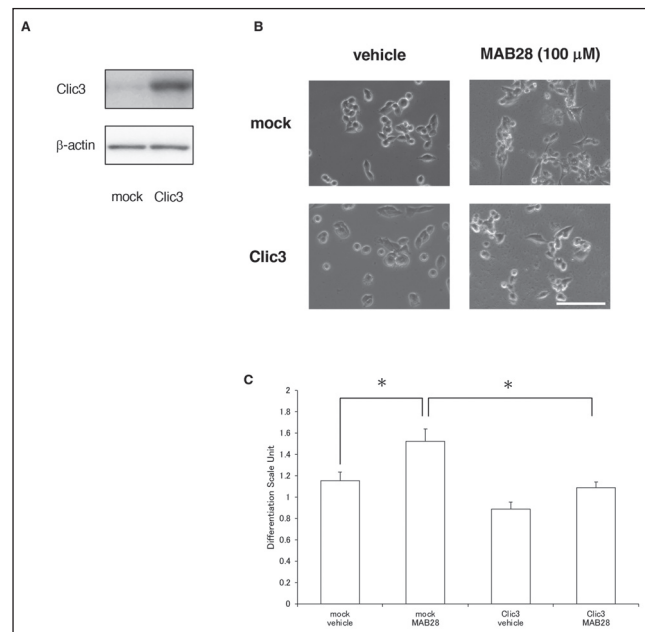


Fig. 7: Effect of overexpression of CLIC3 on MAB28-induced neurite outgrowth in PC12 cells. (A) Western blotting with antibodies against CLIC3 or β -actin was performed. (B) PC12 cells were transfected with vector (mock) or CLIC3. Two days after transfection, the cells were incubated with or without MAB28 (100 μ M) for 2 days, then the differentiation of the cells was evaluated. Scale bar: 100 μ m. (C) Evaluation of differentiation scores of PC12 cells. The differentiation of PC12 cells was evaluated as described in the Experimental section, and the experiments were performed as shown in Fig. 7B. Data are means \pm S.E.M. (n=6). *Significantly different from vehicle at $P < 0.05$.

we aim to investigate the mechanism that triggers ERK activation by MAB28 in future studies.

CLIC3, a type of chloride intracellular channel, also functions as an outward rectifying chloride channel (Kawai et al. 2020). We found that the expression of CLIC3 protein was not affected by NGF but was significantly decreased by stimulation with MAB28 for 2 days. Therefore, it is possible that MAB28 promotes neurite outgrowth by suppressing outward rectifier chloride channel CLIC3 protein expression, which is a different mechanism from that of NGF action. As we assumed that neurite outgrowth is related to the inhibition of chloride ion outflow by chloride channels, we investigated the effects of NPPB, an outward rectifying chloride channel inhibitor, on neurite outgrowth. NPPB significantly increased neurite outgrowth, suggesting that neurite outgrowth by MAB28 stimulation may be related to the inhibition of chloride ion outflow. As the $\text{Na}^+\text{-K}^+\text{-2Cl}^-$ symporter that takes up chloride ions is localized at the tip of neurites in PC12 cells, a higher concentration of chloride ions may appear in the growth cone of the neurite tip than the cell body (Nakajima et al. 2007). Hence, we assumed that MAB28 inhibited the flow of chloride ions out of the cells and increased the concentration of chloride ions inside the cells, which induced neurite outgrowth.

There are no reports that CLIC3 is involved in the activation of ERK, p38MAPK, or CREB. However, Shukla et al. (2016) reported that CLIC4 is essential for the transforming growth factor-beta-induced conversion of fibroblasts to myofibroblasts through the p38MAPK pathway. Arnould et al. (2003) reported that the expression of the mitochondrial chloride intracellular channel (mtCLIC) is dependent on p53 and CREB phosphorylation. Therefore, it would be interesting to clarify how the phosphorylation of ERK, p38MAPK, and CREB is involved in CLIC3 expression.

In summary, we have demonstrated that MAB28 may induce neurite outgrowth by downregulating CLIC3 expression. Further studies are needed to elucidate the precise mechanism of neurite outgrowth induced by MAB28. However, because of its neurite outgrowth promotion, MAB28 may be an effective therapeutic agent for intractable neurological diseases such as neurodegenerative diseases.

4. Experimental

4.1. Materials

Dulbecco's modified Eagle's medium (DMEM) was obtained from Nissui Pharmaceutical Co. Ltd. (Tokyo, Japan), fetal calf serum from Biosera (Cholet, France), and horse serum from Thermo Fisher Scientific (Waltham, MA, USA). Anti-extracellular signal-regulated kinase (ERK), anti-phospho-ERK, anti-p38MAPK, anti-phospho-p38MAPK, anti-CREB, and anti-phospho-CREB antibodies were obtained from Cell Signaling Technology Inc. (Beverly, MA, USA). Anti-CLIC3 antibody was from Proteintech (Rosemont, IL, U.S.A.) and NGF, anti- β -actin antibody, and 5-nitro-2-(3-phenylpropylamino)-benzoic acid (NPPB) were from Sigma Aldrich (Saint Louis, MO, USA). Other chemicals were of reagent grade or the highest quality available.

4.2. General instrumentation

NMR spectra were recorded on a JNM-ECZ500R/S1 (500 MHz for ^1H NMR; 125 MHz for ^{13}C NMR) spectrometer (JEOL, Tokyo, Japan) at 300 K. Chemical shifts are presented as δ values with reference to the internal standard, tetramethylsilane (TMS). Diaion HP-20 porous polymer polystyrene resin (Mitsubishi-Chemical, Tokyo, Japan) and silica gel 60N (63–210 μm particle size, Kanto Chemical, Tokyo, Japan) were used for column chromatography (CC). TLC analysis was performed by using precoated silica gel 60F₂₅₄ or RP18 F₂₅₄S plates (0.25-mm-thick; Merck, Darmstadt, Germany). Compound spots were detected by spraying the TLC plates with $\text{H}_2\text{SO}_4\text{-H}_2\text{O}$ (1:9), followed by heating. Flash chromatography was carried out using a Biotage Isolera™ One system (Biotage, Uppsala, Sweden) with prepacked silica gel columns (Biotage SNAP Ultra 50 g). HPLC was performed using a system consisting of an LC-20AD pump (Shimadzu, Kyoto, Japan), a Rheodyne™ injection port (Thermo Fisher Scientific, Waltham, MA, USA), and an RID-20A detector (Shimadzu). A CHIRAL ART Amylose-SA column (20 mm internal diameter [i.d.] \times 250 mm, 5 μm ; YMC, Kyoto, Japan) was used for preparative HPLC.

4.3. Plant material

Branches of *M. alba* L. cultivated in the medicinal botanical garden of the Takasaki University of Health and Welfare were collected in October 2015. It was identified by one of the authors, K. W. A voucher specimen was deposited in the herbarium of the Takasaki University of Health and Welfare (MA-2015-003).

4.4. Extraction and isolation

The branches of *M. alba* (dry weight, 6.5 kg) were extracted with hot MeOH (2 \times 18 L), and the solvent was removed using an evaporator. The MeOH extract (260 g) was applied to a Diaion HP-20 column and successively eluted with MeOH-H₂O (3:7, 6 L), MeOH-H₂O (3:2, 6 L), MeOH-H₂O (4:1, 6 L), MeOH (6 L), EtOH (3 L), and EtOAc (3 L). The EtOAc-eluted fraction (17.8 g) was subjected to silica gel CC (80 mm i.d. \times 200 mm) eluted with a stepwise gradient mixture of CHCl₃-MeOH (99:1; 9:1; 2:1) and finally with MeOH alone to obtain 13 fractions (frs. A–M). Fraction E was separated by flash chromatography (SNAP Ultra 50 g silica gel column) using Hexane-EtOAc (9:1) as the mobile phase to yield nine fractions (frs. E-1–9). Fraction E-5 was purified by preparative chiral HPLC (20 mm i.d. \times 250 mm) using *n*-hexane-EtOAc (6:1; 9:1) as the mobile phase to obtain 24(R)-ethyllophenol (MAB28) (14.8 mg).

4.5. Cell culture

DMEM containing 10% fetal calf serum, 5% horse serum, 50 units/mL of penicillin, and 50 $\mu\text{g}/\text{mL}$ of streptomycin was used to grow PC12 cells in an incubator under a humidified atmosphere composed of 95% air and 5% CO₂.

4.6. Evaluation of differentiation scores

PC12 cells, seeded at a density of 1×10^5 cells/mL in 6-well plates, were allowed to grow for 3 days before incubation with drugs for 1–2 days. After fixation in 4% paraformaldehyde, PC12 cell morphology was examined using a phase-contrast microscope. PC12 cell neurite outgrowth was considered an index of neuronal differentiation and assigned the following scores: 0 for cells observed no neurite outgrowth; 1 for cells with neurites less than 0.9 times of cell diameter; 2 for cells with neurites 0.9 to 1.1 times of cell diameter; and 3 for cells with neurites longer than 1.1 times of cell diameter (Obara et al. 2001). The averaged scores from about 10 cells were calculated from each well. The final data were expressed from 4 to 5 wells.

4.7. Western blotting

Cells seeded at 1×10^5 cells/mL in 6-well plates were grown for 3 days before overnight incubation with serum-free DMEM followed by incubation with drugs for the indicated times. The supernatant medium was removed and Laemmli sample buffer added before western blotting (Honma et al. 2020). Protein concentration was determined to help normalize the amount of sample to be loaded. The polyvinylidene difluoride membranes to which the resolved proteins were transferred were blocked for 2 h with 0.5% skim milk in Tris-buffered saline containing Tween 20 and then incubated with antibodies against ERK, phospho-ERK, p38MAPK, phospho-p38MAPK, CREB, phospho-CREB, CLIC3, or β -actin. The membranes were then incubated with anti-rabbit horseradish peroxidase-conjugated IgG at 25 °C for 2 h and protein signal detected using an enhanced chemiluminescence assay kit (GE Healthcare UK Ltd., Little Chalfont, United Kingdom) and a luminescent image analyzer (LAS-3000, Fujifilm, Tokyo, Japan). Image Gauge (Fujifilm) was used to quantify the band intensity.

4.8. Real-time reverse transcription-PCR (RT-PCR)

Total RNA was extracted from the cell samples using GenElute Mammalian Total RNA Miniprep kits (Sigma-Aldrich, St. Louis, MO, USA) following the manufacturer's instructions. After cDNA amplification using SYBR Premix Ex Taq (Takara Bio., Otsu, Shiga, Japan), primers specific for WDR18, CLIC3, and INA were used to perform real-time PCR using the PrimePCR system (Bio-Rad). Glyceraldehyde-3-phosphate dehydrogenase (GAPDH) primers were used to measure GAPDH expression: 5'-ACCACAGTCCATGCCATCAC-3' (sense) and 5'-TCCACCACCCTGTTGCTGTA-3' (antisense) (Mitazaki et al. 2011). The real-time PCR conditions were as follows: 95 °C for 2 min, then 30 cycles of 15 s at 95 °C, 30 s at 56 °C, and finally 30 s at 72 °C. mRNA levels of WD repeat domain 18 (WDR18), CLIC3, and internexin neuronal intermediate filament protein alpha (INA) were normalized to GAPDH mRNA levels.

4.9. Transcriptome and proteome analyses

Cells seeded at 1×10^5 cells/mL in 6-well plates were grown for 3 days before overnight incubation with serum-free DMEM followed by incubation with or without MAB28 for 1 day. The supernatant medium was removed and dissolved in ISOGEN. The lysate was outsourced to Kazusa Genome Technologies for transcriptome and proteome analyses. 3'RNA-Seq was used for transcriptome analysis, and data-independent acquisition analysis was used for proteome analysis.

4.10. Transfection

Plasmid pRP[Exp]-EGFP/Puro-CAG>rClc3 and its vector pRP[Exp]-EGFP/Puro-CAG>ORF_stuffer were purchased from VectorBuilder (Chicago, IL, USA). PC12 cells were transfected with the plasmids in accordance with the instructions of the FuGENE 6 Transfection Reagent (Promega). Western blotting was performed to detect the transfection product. Two days after transfection, the cells were incubated with or without MAB28 for 2 days, then the differentiation of the cells was evaluated.

4.11. Protein assays

The bicinchoninic acid assay (Thermo Fisher Scientific, Waltham, MA, USA) was performed to measure protein concentrations; bovine serum albumin was used as the standard.

4.12. Data analysis

The results are expressed as means \pm SEM, and the statistical difference of the values was determined using the Student's *t* test for two-data comparison or one-way of variance with Dunnett's test for multiple comparisons. $P < 0.05$ was considered statistically significant.

Acknowledgments: We thank Yuko Kiyosumi, Mizuki Hyodo, Shoya Tadaki, Harumi Nemoto, Noriyuki Hoshi, Kunihiro Shinomiya, and Takeshi Tadokoro for assistance in the experiments.

Conflict of Interest: The authors have no conflicts of interest to disclose.

References

- Ahn E, Lee J, Jeon YH, Choi SW, Kim E (2017) Anti-diabetic effects of mulberry (*Morus alba* L.) branches and oxyresveratrol in streptozotocin-induced diabetic mice. *Food Sci. Biotechnol* 26: 1693–1702.
- Arnould T, Mercy L, Houbion A, Vankoningsloo S, Renard P, Pascal T, Ninane N, Demazy C, Raes M (2003) mtCLIC is up-regulated and maintains a mitochondrial membrane potential in mtDNA-depleted L929 cells. *FASEB J* 17: 2145–2147.
- Chen M, Zhang S, Wen X, Cao H, Gao Y (2020) Prognostic value of CLIC3 mRNA overexpression in bladder cancer. *PeerJ* 8: e8348.
- Chen PN, Chu SC, Chiou HL, Kuo WH, Chiang CL, Hsieh YS (2006) Mulberry anthocyanins, cyanidin 3-rutinoside and cyanidin 3-glucoside, exhibited an inhibitory effect on the migration and invasion of a human lung cancer cell line. *Cancer Lett* 235: 248–259.
- El-Beshbishy HA, Singab AN, Sinkkonen J, Pihlaja K (2006) Hypolipidemic and antioxidant effects of *Morus alba* L. (Egyptian mulberry) root bark fractions supplementation in cholesterol-fed rats. *Life Sci* 78: 2724–2733.
- Evans SV, Fellows LE, Shing TKM, Fleet GWJ (1985) Glycosidase inhibition by plant alkaloids which are structural analogues of monosaccharides. *Phytochemistry* 24: 1953–1955.
- Gao W, Xu L, Guan R, Liu X, Han Y, Wu Q, Xiao Y, Qi F, Zhu Z, Lin S, Zhang B (2011) Wdr18 is required for Kupffer's vesicle formation and regulation of body asymmetry in zebrafish. *PLoS one* 6: e23386.
- Ginty DD, Bonni A, Greenberg ME (1994) Nerve growth factor activates a Ras-dependent protein kinase that stimulates c-fos transcription via phosphorylation of CREB. *Cell* 77: 713–725.
- Honma S, Tani I, Sakai M, Soma I, Toriyabe K, Yoshida M (2020) Effect of *N*-acetyl Cysteine on renal interstitial fibrosis in mice. *Biol Pharm Bull* 43: 1940–1944.
- Kaplan MP, Chin SS, Fliegner KH, Liem RK (1990) Alpha-internexin, a novel neuronal intermediate filament protein, precedes the low molecular weight neurofilament protein (NF-L) in the developing rat brain. *J Neurosci* 10: 2735–2748.
- Kawai S, Fujii T, Shimizu T, Sukegawa K, Hashimoto I, Okumura T, Nagata T, Sakai H, Fujii T (2020) Pathophysiological properties of CLIC3 chloride channel in human gastric cancer cells. *J Physiol Sci* 70: 15.

- Kim JK, Kim M, Sho SG, Kim MK, Kim SW, Lim YH (2010) Biotransformation of mulberroside A from *Morus alba* results in enhancement of tyrosinase inhibition. *J. Ind. Microbiol Biotechnol* 37: 631–637.
- Marshall CJ (1995) Specificity of receptor tyrosine kinase signaling: transient versus sustained extracellular signal-regulated kinase activation. *Cell* 80: 179–185.
- Mitazaki S, Honma S, Suto M, Kato N, Hiraiwa K, Yoshida M, Abe S (2011) Interleukin-6 plays a protective role in development of cisplatin-induced acute renal failure through upregulation of anti-oxidative stress factors. *Life Sci* 88: 1142–1148.
- Morooka T, Nishida E (1998) Requirement of p38 mitogen-activated protein kinase for neuronal differentiation in PC12 Cells. *J. Biol. Chem* 273: 24285–24288.
- Nakajima K, Miyazaki H, Niisato N, Marunaka Y (2007) Essential role of NKCC1 in NGF-induced neurite outgrowth. *Biochem. Biophys. Res. Commun* 359: 604–610.
- Naowaboot J, Pannangpetch P, Kukongviriyapan V, Kukongviriyapan U, Nakmareong S, Itharat A (2009) Mulberry leaf extract restores arterial pressure in streptozotocin-induced chronic diabetic rats. *Nutr. Res* 29: 602–608.
- Obara Y, Kobayashi H, Ohta T, Ohizumi Y, Nakahata N (2001) Scabronine G-methylester enhances secretion of neurotrophic factors mediated by an activation of protein kinase C-zeta. *Mol. Pharmacol* 59: 1287–1297.
- Shukla A, Yang Y, Madanikia S, Ho Y, Li M, Sanchez V, Cataisson C, Huang J, Yuspa SH (2016) Elevating CLIC4 in Multiple Cell Types Reveals a TGF- β Dependent Induction of a Dominant Negative Smad7 Splice Variant. *PLoS One* 11: e0161410.
- Yamamoto J, Naemura A, Ura M, Ijiri Y, Yamashita T, Kurioka A, Koyama A (2006) Testing various fruits for anti-thrombotic effect: i. Mulberries. *Platelets* 17: 555–564.
- York RD, Yao H, Dillon T, Ellig CL, Eckert SP, McCleskey EW, Stork PJ (1998) Rap1 mediates sustained MAP kinase activation induced by nerve growth factor. *Nature* 392: 622–626.